



Isotopic signatures for natural versus anthropogenic Pb in high-altitude Mt. Everest ice cores during the past 800 years

Khanghyun Lee ^a, Soon Do Hur ^a, Shugui Hou ^{b,c}, Laurie J. Burn-Nunes ^d, Sungmin Hong ^{e,*}, Carlo Barbante ^{f,g}, Claude F. Boutron ^{h,i}, Kevin J.R. Rosman ^{d,1}

^a Korea Polar Research Institute, Songdo Techno Park, 7-50, Songdo-dong, Yeosu-gu, Incheon 406-840, South Korea

^b State Key Laboratory of Cryospheric Science, Cold and Arid Regions Environmental and Engineering Research Institute, Chinese Academy of Science, Lanzhou 730000, China

^c School of Geographic and Oceanographic Sciences, Nanjing University, Nanjing 210093, China

^d Department of Imaging and Applied Physics, Curtin University of Technology, GPO Box U1987, Perth, WA 6845, Australia

^e Department of Ocean Sciences, Inha University, 253 Yonghyun-dong, Nam-gu, Incheon, 402-751, South Korea

^f Department of Environmental Sciences, University Ca'Foscari of Venice, Dorsoduro 2137, 30 123 Venice, Italy

^g Institute for the Dynamics of Environmental Processes–CNR, University Ca'Foscari of Venice, Dorsoduro 2137, 30 123 Venice, Italy

^h Laboratoire de Glaciologie et Géophysique de l'Environnement (UMR Université Joseph Fourier/CNRS 5183), 54 rue Molière, BP 96, 38402 Saint Martin d' Hères Cedex, France

ⁱ Unité de Formation et de Recherche "Physique, Ingénierie, Terre, Environnement, Mécanique", Université Joseph Fourier de Grenoble (Institut Universitaire de France), 715 rue de la Houille Blanche, BP 53, 38041 Grenoble Cedex 9, France

ARTICLE INFO

Article history:

Received 21 July 2011

Received in revised form 3 October 2011

Accepted 4 October 2011

Available online 1 November 2011

Keywords:

Pb isotopes

Ice cores

Mt. Everest

Anthropogenic Pb contamination

Leaded gasoline

South Asia

ABSTRACT

A long-term record, extending back 800 years (1205 to 2002 AD), of the Pb isotopic composition ($^{206}\text{Pb}/^{207}\text{Pb}$ and $^{208}\text{Pb}/^{207}\text{Pb}$) as well as Pb concentrations from high altitude Mt. Everest ice cores has the potential to identify sources and source regions affecting natural and anthropogenic Pb deposition in central Asia. The results show that the regional natural background Pb isotope signature (~ 1.20 for $^{206}\text{Pb}/^{207}\text{Pb}$ and ~ 2.50 for $^{208}\text{Pb}/^{207}\text{Pb}$) in the central Himalayas was dominated by mineral dust over the last ~ 750 years from 1205 to 1960s, mostly originating from local sources with occasional contributions of long-range transported dust probably from Sahara desert and northwestern India. Since the 1970s, the Pb isotope ratios are characterized by a continuous decline toward less radiogenic ratios with the least mean ratios of 1.178 for $^{206}\text{Pb}/^{207}\text{Pb}$ and 2.471 for $^{208}\text{Pb}/^{207}\text{Pb}$ in the period 1990–1996. The depression of the $^{206}\text{Pb}/^{207}\text{Pb}$ and $^{208}\text{Pb}/^{207}\text{Pb}$ values during the corresponding periods is most likely due to an increasing influence of less radiogenic Pb of anthropogenic origin mainly from leaded gasoline used in South Asia (India as well as possibly Bangladesh and Nepal). From 1997 to 2002, isotopic composition tends to show a shift to slightly more radiogenic signature. This is likely attributed to reducing Pb emissions from leaded gasoline in source regions, coinciding with the nationwide reduction of Pb in gasoline and subsequent phase-out of leaded gasoline in South Asia since 1997. An interesting feature is the relatively high levels of Pb concentrations and enrichment factors (EF) between 1997 and 2002. Although the reason for this feature remains uncertain, it would be probably linked with an increasing influence of anthropogenic Pb emitted from other sources such as fossil fuel combustion and non-ferrous metal production.

© 2011 Elsevier B.V. All rights reserved.

1. Introduction

Recently, century-scale records of changes in the occurrence of various trace elements (Cu, Zn, As, Mo, Cd, Sn, Sb, Cs, Pb, Bi, and U) in high altitude Mt. Everest ice cores in the central Himalayas have led to a growing understanding of anthropogenic influence on the biogeochemical cycle of these elements in high altitude atmosphere in central Asia (Hong et al., 2009, submitted for publication; Kaspari et al., 2009). Such records demonstrated a legacy of trace element contamination in recent decades, suggesting a possible influence of

emissions in South Asia for Cu, Zn, As, Mo, Cd, Sn, Sb and Pb (Hong et al., 2009, submitted for publication) or either regional or global emissions for Cs, Bi, and U (Kaspari et al., 2009). Although the long-range atmospheric transport is undoubtedly recognized as an important source of trace element contamination in the central Himalayas, however, the potential source regions remain substantially poorly understood. This is because previous studies evaluated source regions using the similarities and differences in temporal trends between ice cores and emission inventories of trace elements in various countries and even regions as well as wind regimes prevailing in the Himalayas.

Over the last decades, the isotopic composition (^{204}Pb , ^{206}Pb , ^{207}Pb and ^{208}Pb) of Pb in the atmosphere of the Northern Hemisphere has been used as a potential tracer of identifying aerosol provenance

* Corresponding author. Tel.: +82 32 8607708.

E-mail address: smhong@inha.ac.kr (S. Hong).

¹ This paper is dedicated to the memory of K.J.R. Rosman.

and providing insight into the pathways of pollution transport from source to a receptor in association with atmospheric circulation pattern (Komárek et al., 2008). Using the characteristics of Pb isotopes that varies as a consequence of the emissions and dispersion of Pb from anthropogenic sources, the temporal changes in Pb isotopes from environmental archives such as snow and ice have greatly helped to trace the changing major sources and source regions of anthropogenic Pb introduced into either regional or global environment primarily through atmospheric transport over time (e.g., Rosman et al., 1993, 1994, 1997; Schwikowski et al., 2004; Shotykh et al., 2005; Zheng et al., 2007). For instance, the Greenland snow and ice archives showed a shift of $^{206}\text{Pb}/^{207}\text{Pb}$ ratio to lower values (~ 1.18) during the Roman times between 400 B.C. and 300 A.D. from ~ 1.20 in ~ 8 -kyr-old pre-anthropogenic ice (Rosman et al., 1997). This provided unequivocal evidence that early large-scale atmospheric Pb pollution is of anthropogenic origin. Isotopic systematics between $^{206}\text{Pb}/^{207}\text{Pb}$ and $^{208}\text{Pb}/^{207}\text{Pb}$ demonstrated that most of the Pb originated from the mining districts in Iberian Peninsula during the corresponding time period. More recently, the extensive use of Pb additives in gasoline since the 1930s has led to the greatest recorded levels of Pb pollution occurring during the mid-20th century (Murozumi et al., 1969; Boutron et al., 1991; Candelone et al., 1995). The studies of Pb isotopic patterns in Greenland snow were satisfactorily used to the sources and dispersal of gasoline-derived Pb, showing that the $^{206}\text{Pb}/^{207}\text{Pb}$ ratio increased from 1960s (~ 1.16), reaching a peak value (~ 1.18) between 1975 and 1980, and then declined to its earlier values by the mid-1980s (Rosman et al., 1993, 1994). Such change was attributed to different contributions from the deposition of more radiogenic Pb from the United States, and relatively constant levels of Pb from Eurasia arriving to central Greenland during the three decades between 1960 and 1988. Apart from long-term Pb isotopic patterns, seasonal resolution gave more characterized record of the specific Pb pollution sources attributing to the variation of Pb isotope ratios in consistent with Pb enrichment factors with respect to the background in Greenland snow and ice (Rosman et al., 1998).

Hong et al. (submitted for publication) have reported a long-term record (1205 to 2002 AD) of Pb and Sc concentrations from Mt. Everest ice cores using Inductively Coupled Plasma Mass Spectrometry (ICP-MS). They found that Pb aerosol in the remote Himalayan atmosphere was primarily of natural origin until the mid-20th century. In contrast, the Pb enrichment factors normalized by Sc concentrations showed a significant increase from the 1970s onwards, which was attributed to atmospheric Pb of anthropogenic origin from South Asia, combining preliminary $^{206}\text{Pb}/^{207}\text{Pb}$ ratios determined in selected samples by thermal ionization mass spectrometry (TIMS).

However, source apportionment of Pb pollution as well as natural Pb contributed predominantly from rock and soil dust has not been reported, because of no full measurements of Pb isotope abundance in the samples analyzed for Pb concentrations.

Here we present the first comprehensive record of the $^{206}\text{Pb}/^{207}\text{Pb}$ and $^{208}\text{Pb}/^{207}\text{Pb}$ ratios determined from Mt. Everest ice cores, spanning the last 800 years from 1205 to 2002 AD, by means of TIMS. Mt. Everest is located at the boundary of the South Asian monsoon and the continental climate of central Asia, which represents an ideal environment for studying changes in the atmospheric composition over central Asia (Fig. 1). As maritime air masses move from the Indian Ocean during the summer monsoon season, monsoon precipitation accounts for the bulk of the annual precipitation in the Himalayas (Thompson et al., 2000). The purpose of this study is to establish the first continuous, long-term chronological variations in Pb isotopic composition in the high-altitude atmosphere of central Himalayas. This will enable to identify the origin of natural Pb during preindustrial time and to estimate the potential sources and source regions of anthropogenic Pb affecting atmospheric Pb composition in central Asia. In addition, as the Himalayan region is strongly influenced by the monsoon regime, our data would provide a valuable opportunity to evaluate the anthropogenic influence on the atmospheric environment of this region in response to rapid economic and industrial developments in South Asia.

2. Material and methods

2.1. Ice core samples and decontamination

Ice core samples were taken from two firn/ice cores: 108.8 m [ER-a] and 95.8 m [ER-b] recovered from the East Rongbuk (ER) glacier on the northeast slope of Mt. Everest ($28^{\circ}03'\text{N}$, $86^{\circ}96'\text{E}$, 6518 m asl) in 2002 (Fig. 1). A total of 102 sections with lengths between 20 and 65 cm were selected from half cross-sections of ER-a and ER-b ice cores and transported frozen to the Korea Polar Research Institute (KOPRI).

Dating of the ER-a core was performed by combining several methods: the counting annual layers down to a depth of 98 m (1534 AD); the identification of major volcanic events using peaks of Bi; and the use of a flow model below a depth of 98 m due to layer thinning (Kaspari et al., 2007, 2008; Xu et al., 2009a). Dating uncertainties are ± 0 year at 1963 AD and ± 5 year at 1534 AD. More details are given in Kaspari et al. (2007, 2008) and Xu et al. (2009a). The resulting time scale of the ER-a core was applied directly to the ER-b core, which rendered uncertainty within 1 year or less (Hong et al., 2009). The core sections from ER-b core covered

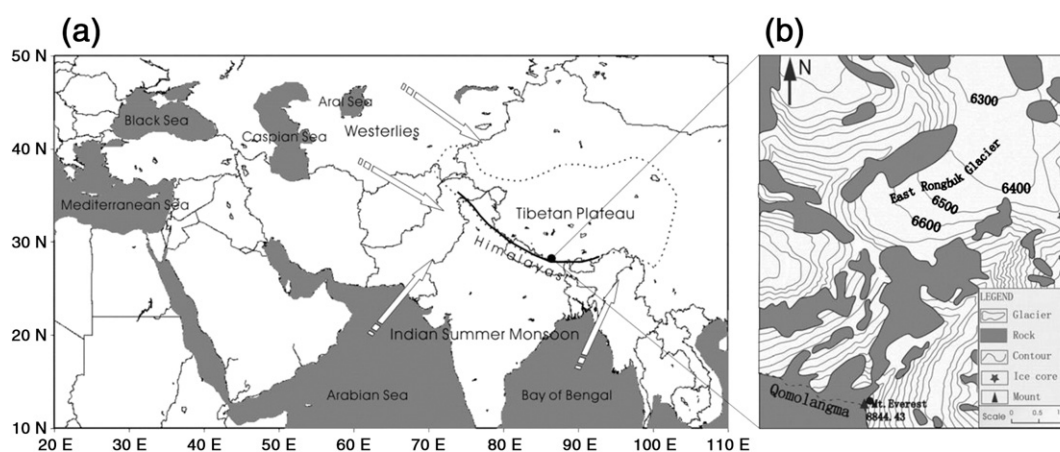


Fig. 1. (a) The study area in the central Himalayas and general patterns for winter and summer circulation systems. The thick line represents the northern border of the summer monsoon (34° – 35°N in the middle of the plateau). (b) Map of the Mt. Everest ice core drilling site.

the period from 1971 to 2002 and sections of the ER-a core covered the pre-1970 period (Table 1).

Each core section was decontaminated at KOPRI by mechanical removal of successive layers of ice from the outside to the innermost part of the section using ultra-clean procedures (Candelone et al., 1994; Hong et al., 2000). The inner core so obtained was either collected whole or, if longer than 20-cm, was cut into several successive parts. The time resolution of the samples varied integrating one month to several months in the upper ~50 m (dated from the 1900s) and slightly less or more than one year below ~50 m, depending on the length of inner core analyzed. Decontaminated samples were melted at room temperature inside class 10 clean benches in a class 1000 clean room at KOPRI. About 10 mL of aliquots were then taken in acid-cleaned 15 mL low-density polyethylene (LDPE) bottles (Hong et al., 2000), frozen and transported to Curtin University in Perth, Australia, for analysis.

2.2. Analytical procedures

The measurements were carried out using a VG354 magnetic sector field, multi-collector, Thermal Ionization Mass Spectrometer (Fisons Instruments) at Curtin University. Details of the preparation and analysis of the samples have been described by Vallelonga et al. (2002 and references therein). Briefly, samples were melted and aliquots of ~3 mL were transferred to a preconditioned Teflon beaker containing 10 μL of nitric acid (HNO_3), 20 μL of hydrofluoric acid (HF), 4 μL of dilute phosphoric acid (H_3PO_4 , approximately 5% by weight), and 10 μL of a ^{205}Pb spike solution. The solution was then evaporated to dryness at sub-boiling temperature. The evaporated residue was then transferred in a droplet of a silicic acid silica gel/phosphoric acid ionization enhancer to an acid-cleaned zone-refined rhenium mass spectrometer filament and dried by passing an electric current through the filament. Addition of the ^{205}Pb enriched tracer to the sample enabled the determination of both the Pb concentrations by isotope dilution mass spectrometry (IDMS) and Pb isotopes (^{204}Pb , ^{205}Pb , ^{206}Pb , ^{207}Pb , and ^{208}Pb) in the same analysis (Chisholm et al., 1995). The regular measurement of the NIST SRM981 showed that there was a bias of ~0.2% in the ^{208}Pb isotope abundance, which is smaller than the precision reported here.

3. Results

3.1. Pb concentrations in the ice record

Lead concentrations in 151 depth intervals are presented in Table 1 and displayed in Fig 3a. Lead was previously measured in our samples using Inductively Coupled Plasma Mass Spectrometry (ICP-MS) (Perkin Elmer Sciex, ELAN 6000), with repeatability in the measurements found to be ~12% (Hong et al., submitted for publication). Fig. 2 shows the comparison between the results obtained by the two techniques. The Pb concentrations from both methods are in a fairly good agreement with Pearson's correlation coefficients of 0.92 for all data and 0.81 for Pb concentrations less than 100 pg g^{-1} , respectively, that are significant at $p = 0.01$. However, the ICP-MS Pb data are shown to be systematically lower (slopes of 0.67 for all data and 0.75 for Pb values less than 100 pg g^{-1}). Such difference was also observed for Pb concentrations obtained from Antarctic snow by single collector sector field ICP-MS (ICP-SFMS) and TIMS (Planchon et al., 2001). The lower ICP-MS Pb concentration levels are probably due to incomplete vaporization and atomization of a small number of larger particles when the particles in the samples are transferred into the ICP. The slope of the correlation line between Pb concentrations from both methods is better (Fig. 2) when the TIMS Pb data larger than 100 pg g^{-1} are excluded, suggesting that the difference between the Pb data from both methods appears substantially to be due to the particles in the samples. Additionally, difference in acid

Table 1

Pb concentrations, Pb isotopic composition and crustal enrichment factors determined in 151 depth intervals from Mt. Everest ice cores.

Depth interval (m)		Estimated bottom age	Pb (pg g^{-1})	$^{206}\text{Pb}/^{207}\text{Pb}$	U^a	$^{208}\text{Pb}/^{207}\text{Pb}$	U^a	crustal EF ^b
Top	Bottom							
1.30	1.40	2001.9	82	1.1616	0.0022	2.4475	0.0025	9.7
2.40	2.52	2001.0	44	1.1807	0.0034	2.4766	0.0050	3.3
2.60	2.71	2000.9	87	1.1928	0.0014	2.4874	0.0040	3.1
2.97	3.14	2000.5	66	1.1854	0.0027	2.4791	0.0036	3.9
3.34	3.46	2000.1	61	1.1879	0.0031	2.4887	0.0057	3.9
4.29	4.39	1998.9	5.0	1.1735	0.0047	2.4673	0.0107	2.1
4.63	4.74	1998.7	54	1.1917	0.0043	2.4900	0.0046	1.9
5.25	5.38	1997.9	57	1.1837	0.0035	2.4712	0.0059	2.7
5.68	5.81	1997.5	504	1.1807	0.0033	2.4726	0.0044	2.6
5.93	6.05	1997.0	71	1.1813	0.0021	2.4619	0.0062	3.6
6.17	6.38	1996.8	58	1.1710	0.0012	2.4580	0.0030	4.2
6.47	6.55	1996.6	26	1.1792	0.0028	2.4729	0.0055	2.1
6.55	6.72	1996.5	133	1.1777	0.0045	2.4654	0.0094	1.7
6.84	6.94	1996.2	50	1.1750	0.0037	2.4654	0.0063	6.3
6.94	7.05	1996.0	48	1.1712	0.0025	2.4563	0.0057	5.2
7.21	7.34	1995.7	22	1.1656	0.0044	2.4511	0.0051	9.6
7.62	7.74	1995.4	206	1.1702	0.0040	2.4551	0.0060	4.0
7.84	7.97	1995.0	48	1.1885	0.0048	2.4902	0.0083	2.7
7.97	8.08	1994.9	30	1.1829	0.0040	2.4693	0.0068	4.4
8.19	8.46	1994.6	24	1.1730	0.0018	2.4650	0.0040	10.1
8.57	8.61	1994.4	82	1.1763	0.0034	2.4628	0.0045	7.4
8.61	8.65	1994.3	36	1.1874	0.0036	2.4881	0.0080	9.4
8.65	8.69	1994.3	15	1.1774	0.0058	2.4762	0.0098	5.8
8.69	8.73	1994.2	22	1.1826	0.0036	2.4724	0.0097	3.8
8.73	8.77	1994.2	8.9	1.1565	0.0052	2.4470	0.0102	6.9
8.77	8.81	1994.1	31	1.1757	0.0028	2.4592	0.0076	12.1
8.81	8.86	1994.1	50	1.1918	0.0032	2.4946	0.0084	1.9
8.86	8.91	1994.0	19	1.1737	0.0048	2.4697	0.0099	6.3
8.91	8.96	1994.0	13	1.1586	0.0046	2.4539	0.0094	6.1
8.96	9.01	1994.0	11	1.1803	0.0105	2.5099	0.0155	0.9
9.01	9.05	1993.9	5.8	1.2142	0.0214	2.5016	0.0457	2.4
9.28	9.33	1993.6	335	1.1855	0.0020	2.4805	0.0035	4.8
9.33	9.38	1993.6	287	1.1765	0.0041	2.4670	0.0056	2.2
9.38	9.43	1993.5	32	1.1602	0.0038	2.4469	0.0064	0.8
9.43	9.48	1993.5	39	1.1606	0.0031	2.4465	0.0059	4.1
9.68	9.81	1992.7	57	1.2013	0.0030	2.4999	0.0036	1.4
9.94	10.08	1992.3	51	1.1779	0.0031	2.5037	0.0084	4.4
10.23	10.40	1991.9	21	1.1722	0.0028	2.4597	0.0061	4.1
10.51	10.69	1991.6	70	1.1772	0.0030	2.4672	0.0061	5.3
10.79	10.91	1991.5	24	1.2197	0.0040	2.5071	0.0098	3.2
11.03	11.27	1991.0	31	1.1750	0.0039	2.4590	0.0050	3.4
11.39	11.49	1990.6	482	1.1909	0.0033	2.4860	0.0043	2.9
11.49	11.62	1990.4	10	1.1578	0.0033	2.4451	0.0079	10.4
11.62	11.76	1990.1	14	1.1799	0.0051	2.4751	0.0074	5.5
12.06	12.21	1989.7	277	1.1805	0.0017	2.4739	0.0044	4.0
12.30	12.47	1989.3	8	1.1577	0.0077	2.4465	0.0084	2.0
12.47	12.64	1989.1	47	1.1878	0.0025	2.4852	0.0056	2.4
12.75	12.88	1988.7	9.6	1.1599	0.0067	2.4535	0.0110	1.0
13.00	13.20	1988.0	28	1.1780	0.0027	2.4670	0.0030	8.3
13.33	13.51	1987.7	316	1.1913	0.0021	2.4843	0.0052	5.4
14.74	14.95	1986.2	412	1.1985	0.0047	2.4941	0.0057	3.4
14.98	15.28	1985.9	46	1.1920	0.0023	2.4900	0.0040	1.9
16.54	16.73	1983.8	33	1.1776	0.0028	2.4678	0.0059	2.2
17.01	17.23	1983.0	19	1.1810	0.0114	2.4640	0.0280	6.3
17.89	18.02	1981.9	31	1.1817	0.0041	2.4713	0.0063	1.4
8.02	18.15	1981.8	19	1.1858	0.0046	2.4804	0.0074	4.0
18.30	18.40	1981.6	85	1.1994	0.0030	2.4988	0.0081	2.0
18.40	18.56	1981.5	96	1.1866	0.0021	2.4787	0.0044	2.2
19.19	19.34	1980.7	41	1.1813	0.0022	2.4651	0.0040	2.5
19.34	19.49	1980.5	264	1.1912	0.0019	2.4900	0.0040	2.3
20.33	20.53	1979.2	105	1.1908	0.0025	2.4768	0.0046	2.3
21.14	21.48	1978.2	65	1.1810	0.0021	2.4710	0.0030	4.5
22.71	22.89	1976.8	7.7	1.1850	0.0071	2.4946	0.0092	1.5
23.65	23.85	1975.9	35	1.1990	0.0020	2.4970	0.0030	7.5
25.11	25.16	1974.6	28	1.1854	0.0034	2.4701	0.0061	3.6
25.16	25.21	1974.4	98	1.1860	0.0034	2.4806	0.0043	2.9
25.21	25.26	1974.2	305	1.1853	0.0019	2.4815	0.0062	4.2
25.26	25.31	1974.0	106	1.1899	0.0044	2.4859	0.0065	1.3
25.31	25.36	1973.9	145	1.1902	0.0040	2.4868	0.0055	5.1
25.36	25.41	1973.9	29	1.1876	0.0040	2.4882	0.0060	3.1
25.41	25.46	1973.8	55	1.1998	0.0032	2.4976	0.0075	1.5
25.46	25.51	1973.7	14	1.1914	0.0063	2.4861	0.0089	8.1

Table 1 (continued)

Depth interval (m)		Estimated bottom age	Pb (pg g ⁻¹)	²⁰⁶ Pb/ ²⁰⁷ Pb	U ^a	²⁰⁸ Pb/ ²⁰⁷ Pb	U ^a	crustal EF ^b
Top	Bottom							
25.51	25.56	1973.6	7.6	1.1963	0.0073	2.5014	0.0129	3.6
25.56	25.61	1973.6	101	1.1912	0.0037	2.4854	0.0068	3.8
25.61	25.66	1973.5	98	1.1862	0.0014	2.4782	0.0055	4.3
26.26	26.39	1972.2	40	1.2065	0.0091	2.4956	0.0094	1.9
26.39	26.53	1971.9	61	1.1932	0.0050	2.4911	0.0088	2.8
26.56	26.71	1966.0	241	1.1971	0.0012	2.4845	0.0036	2.4
26.71	26.85	1965.8	39	1.1975	0.0008	2.4936	0.0027	3.4
26.90	27.01	1965.7	83	1.1978	0.0010	2.4920	0.0037	1.0
27.01	27.12	1965.5	47	1.1987	0.0023	2.4951	0.0057	2.0
27.12	27.23	1965.4	225	1.2007	0.0020	2.4971	0.0016	1.8
27.23	27.34	1965.3	90	1.1963	0.0024	2.4890	0.0029	2.7
28.59	28.77	1963.5	29	1.1856	0.0033	2.4767	0.0107	3.0
30.98	31.21	1959.9	130	1.2006	0.0022	2.4948	0.0120	2.3
31.21	31.43	1959.6	64	1.2032	0.0019	2.5158	0.0023	2.4
32.98	33.18	1957.2	45	1.1954	0.0040	2.4987	0.0056	1.2
36.73	36.91	1950.0	15	1.1968	0.0050	2.4922	0.0126	2.3
36.91	37.09	1949.7	16	1.1980	0.0057	2.5026	0.0111	1.6
38.28	38.57	1946.5	108	1.1962	0.0027	2.4904	0.0033	2.9
39.60	39.75	1944.3	49	1.2040	0.0033	2.4983	0.0081	1.4
39.75	39.90	1943.9	44	1.2036	0.0022	2.5016	0.0038	3.4
41.85	42.03	1936.9	124	1.1996	0.0013	2.4975	0.0055	2.1
42.03	42.22	1936.2	75	1.1983	0.0020	2.4929	0.0057	2.2
44.01	44.28	1928.1	13	1.2097	0.0026	2.5053	0.0028	4.1
46.20	46.38	1921.1	96	1.1997	0.0020	2.4991	0.0045	1.9
50.36	50.51	1901.4	47	1.2068	0.0053	2.5053	0.0116	1.8
50.66	50.81	1900	39	1.1998	0.0036	2.5009	0.0061	1.7
50.81	50.96	1899	8.0	1.2019	0.0020	2.5055	0.0050	2.9
51.05	51.30	1897	54	1.2068	0.0022	2.5012	0.0323	1.8
51.36	51.53	1896	78	1.2045	0.0025	2.5006	0.0075	2.4
53.98	54.26	1879	16	1.1939	0.0017	2.4906	0.0039	2.1
56.14	56.43	1864	61	1.1912	0.0029	2.4860	0.0059	1.4
60.74	61.04	1838	33	1.2023	0.0035	2.5008	0.0080	1.7
61.12	61.46	1835	55	1.2117	0.0031	2.4991	0.0039	1.7
61.56	61.75	1833	85	1.2032	0.0040	2.4977	0.0078	2.2
64.03	64.40	1820	109	1.2035	0.0040	2.5006	0.0080	2.5
66.00	66.30	1810	44	1.1995	0.0023	2.5075	0.0049	1.9
69.16	69.32	1792	62	1.1975	0.0020	2.4927	0.0047	1.7
69.32	69.48	1791	99	1.1980	0.0042	2.4879	0.0072	1.9
105.60	105.67	1205	22	1.2020	0.0010	2.5010	0.0030	1.9

^a Uncertainties are 95% confidence intervals.

^b Crustal enrichment factors for Pb, calculated with Sc as a crustal reference metal (see text).

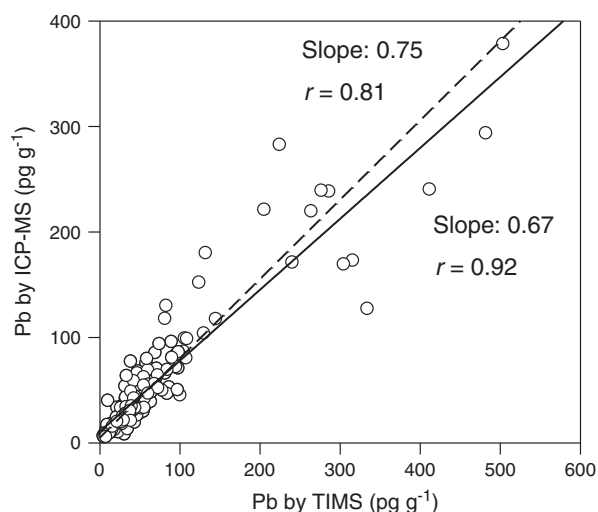


Fig. 2. Comparison of Pb concentrations determined by ICP-MS and TIMS. Linear regression lines are represented by solid line for all measured concentrations and dashed line for the data excluding more than 100 pg g⁻¹ of Pb by TIMS, respectively.

digestion procedures between the two analytical techniques could also be attributed to the different concentration levels measured by both methods. The samples were acid-digested with a mixture of HNO₃, HF and H₃PO₄ for analysis by TIMS (Vallelonga et al., 2002), whereas aliquots for analysis by ICP-MS were acidified to 1% with HNO₃ (Lee et al., 2008). The acid leaching procedure using different reagents (especially HF) for TIMS analysis may provide more efficient dissolution of silica-based particles (Dean, 2003), which, in turn, result in the higher TIMS Pb concentration levels with respect to the ICP-MS Pb concentrations. Despite systematic difference between the ICP-MS Pb and TIMS Pb, we use the TIMS Pb data in this study, because the Pb concentrations and Pb isotopic compositions were determined in the same analysis.

As observed in previous study, the data indicate two periods of Pb concentrations, pre-1960s where Pb concentrations show relatively small variations and post-1960s where a striking increase and large variability in concentrations of Pb are shown (Fig. 3a). A strong variability in recent decades is primarily likely due to the seasonal variations, because the time resolution of the samples during a corresponding period integrates one month to several months. It is well documented in high altitude Himalayan snow and ice that the concentrations of trace elements are generally enhanced in winter–spring due to increase in atmospheric dust input from central Asia, and the concentrations tend to decrease in the summer monsoon season as a result of massive moisture supply from the Indian Ocean and increased regional precipitation, both of which can dilute the concentration levels of trace elements (Lee et al., 2008; Hong et al., 2009; Kaspari et al., 2009).

The mean concentrations in different time periods are summarized in Table 2. To facilitate comparisons, the pre-1900 period was chosen as a reference because the concentrations remain relatively constant and anthropogenic inputs are expected to be potentially negligible (Hong et al., 2009; Kaspari et al., 2009). The post-1900 specific time periods were chosen to evaluate possible differences in the major sources contributing to the changes in Pb deposition as described below. In Table 2, more than two-fold increase in Pb concentrations occurs in the 1960s, 1980s, and 1997–2002.

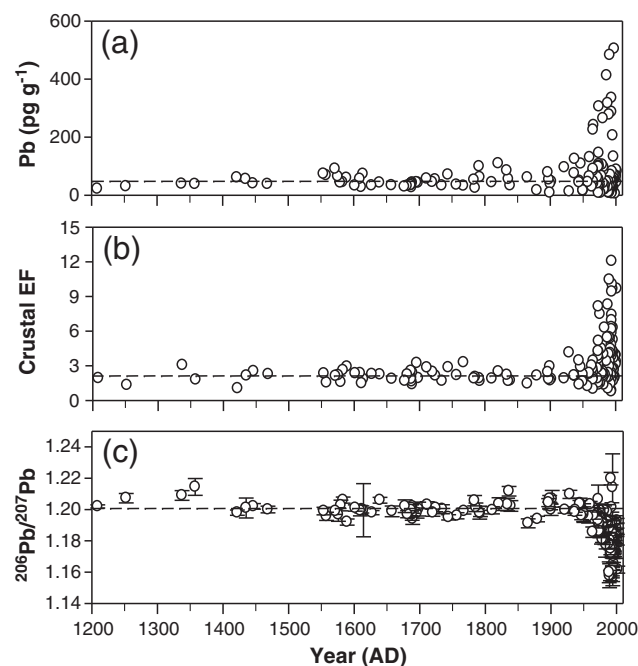


Fig. 3. Changes in Pb concentrations, crustal enrichment factors, and ²⁰⁶Pb/²⁰⁷Pb ratios in Mt. Everest ice cores over the past 800 years. Dashed line represents the mean value for the pre-1900. Uncertainties for ²⁰⁶Pb/²⁰⁷Pb ratios are 95% confidence intervals.

Table 2
Mean values of Pb concentrations (in pg g^{-1}) and crustal enrichment factors (EF) with one standard deviation, and isotopic ratios over the post-1900 specific time periods and pre-1900. Increase factor (IF) between separated time periods and the pre-1900 mean values are also presented. Uncertainties for the isotope ratios are 95% confidence intervals.

Period	Pb		EFs		$^{206}\text{Pb}/^{207}\text{Pb}$	$^{208}\text{Pb}/^{207}\text{Pb}$	n^a
	Mean \pm SD	IF	Mean \pm SD	IF			
1997–2002	103 \pm 142	2.1	3.7 \pm 2.2	1.8	1.182 \pm 0.003	2.474 \pm 0.005	10
1990–1996	70 \pm 104	1.5	4.9 \pm 2.9	2.3	1.178 \pm 0.004	2.471 \pm 0.008	34
1980s	108 \pm 130	2.3	3.2 \pm 2.0	1.5	1.183 \pm 0.004	2.476 \pm 0.007	16
1970s	77 \pm 72	1.6	3.7 \pm 1.9	1.8	1.191 \pm 0.004	2.486 \pm 0.007	17
1960s	111 \pm 82	2.3	2.3 \pm 0.8	1.1	1.197 \pm 0.002	2.490 \pm 0.005	8
1900–1959	57 \pm 36	1.2	2.2 \pm 0.8	1.0	1.201 \pm 0.003	2.500 \pm 0.006	13
Before 1900	48 \pm 21	–	2.1 \pm 0.5	–	0.201 \pm 0.003	2.497 \pm 0.006	53

^a Number of samples analyzed.

3.2. Pb isotopic composition in the ice record

The Pb isotope ratios determined in the ice cores are given in Table 1. Figs. 3c and 4 show changes in $^{206}\text{Pb}/^{207}\text{Pb}$ ratios over time and the plot of $^{206}\text{Pb}/^{207}\text{Pb}$ versus $^{208}\text{Pb}/^{207}\text{Pb}$, respectively. The $^{206}\text{Pb}/^{207}\text{Pb}$ ratios do not significantly vary in the pre-1900 period with an average of 1.201. The mean ratio remains very similar until 1950s (Table 2). The Pb isotope ratios then show a decline to less radiogenic values from the 1960s, reaching a maximum drop of mean ratios down to 1.178 in the period 1990–1996 (Table 2 and Fig. 3c), while Pb concentrations are observed to increase during a corresponding period. In recent years, the ratios became slightly more radiogenic.

4. Discussion

4.1. Natural versus anthropogenic lead deposition to the central Himalayas

The airborne mineral dust is regarded as the major contributor of the natural background Pb to the atmosphere of the Northern Hemisphere, except for the time periods, during which the inputs of Pb from either large volcanic eruptions or anthropogenic source are added (Hong et al., 1994; Zheng et al., 2007). To characterize anthropogenic Pb inputs from Pb of natural origin in the ice cores, the Pb enrichment factors (EF) relative to soils (<20 μm fractions) of the Tibetan Plateau, one of the most significant dust source regions in central Asia (Li et al., 2009), were normalized to the Pb/Sc ratio ($\text{EF} = (\text{Pb}/\text{Sc})_{\text{ice}}/(\text{Pb}/\text{Sc})_{\text{soil}}$), using Sc as a reference metal for mineral dust, which were previously measured in the same samples (Hong et al., submitted for publication). The uncertainty in EF calculation is primarily attributed to the differences between elemental compositions of local soil and reference crustal composition.

The EFs are characterized by low value (mean value of ~ 2) for the pre-1900 period and remains very constant until the 1960s (Table 2 and Fig. 3b). When compared to the mean EF values (~ 1) for the ICP-MS Pb data during the corresponding time period in previous study (Hong et al., submitted for publication), rather high EF values are observed for the TIMS Pb. This is of course due to the systematically higher TIMS Pb data in comparison with the ICP-MS Pb as discussed in Section 3.1. No significant enrichment of Pb during this period reflects that mineral dust as the primary source dominated the input of Pb in the central Himalayas without an influence of human-induced Pb during the last ~ 750 years from 1205 to 1960s (Hong et al., submitted for publication).

Since the 1970s, an increasing trend of EF values is shown with a peak (mean value of 2.3) in the mid-1990s. A slight decrease is then observed in the period 1997–2002. A significant increase in EFs coupled with reduced radiogenic $^{206}\text{Pb}/^{207}\text{Pb}$ values gives evidence of anthropogenic Pb enrichment in recent decades (Fig. 3c). For comparison, long-distance atmospheric transport of Pb from mid- and low-latitude sources to the most remote areas in the Northern Hemisphere has resulted in a large-scale Pb contamination since the Industrial Revolution and especially since the 1930s, from which gasoline

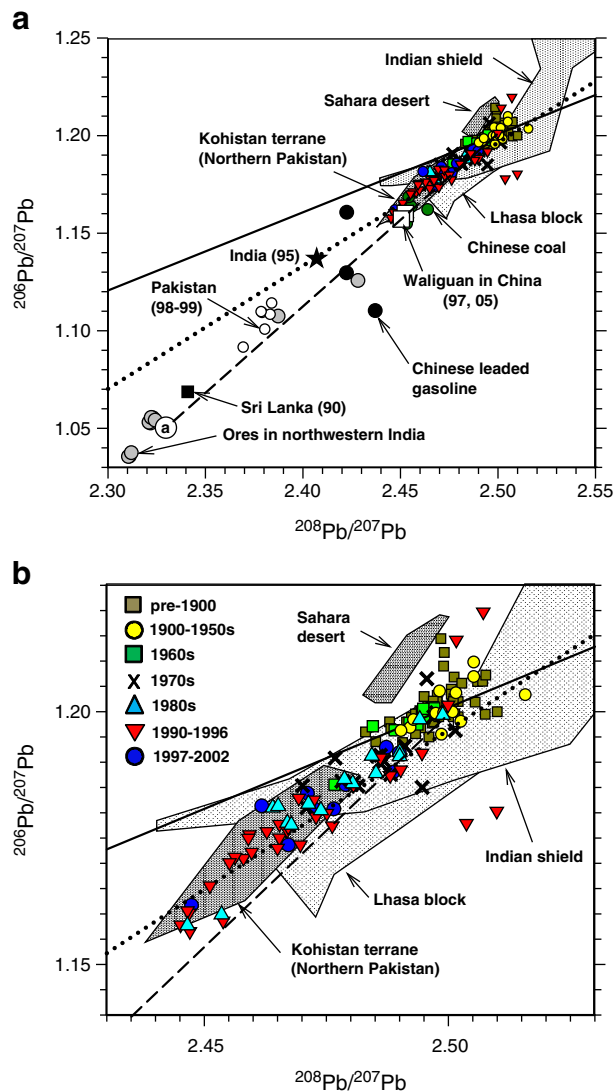


Fig. 4. $^{208}\text{Pb}/^{207}\text{Pb}$ versus $^{206}\text{Pb}/^{207}\text{Pb}$ in the depth intervals from 1205 to 2002 AD: (a) source @ typical for Australian Pb ores with low radiogenic $^{206}\text{Pb}/^{207}\text{Pb}$ ($^{208}\text{Pb}/^{207}\text{Pb}$ ratios of 1.04 (2.32) (Cummings and Richards, 1975), the areas indicating the range of Pb isotopic compositions of K-feldspars of Indian shield (Gariépy et al., 1985), Lhasa Block (Gariépy et al., 1985), rocks in Kohistan terrane of northern Pakistan Himalaya (Khan et al., 1997), soils in Sahara Desert (Sun, 1980). Also included are Pb isotopic compositions in aerosols of India (Bollhöfer and Rosman, 2001), Pakistan (Bollhöfer and Rosman, 2001), Sri Lanka (Mukai et al., 1993), and China (Mukai et al., 2001; Cheng et al., 2007), Indian Pb ores (Deb et al., 1989), Chinese coals (Chen et al., 2005; Díaz-Somoano et al., 2009), Chinese leaded gasoline (Zhu et al., 2001; Tan et al., 2006). A dashed line connects two end points of Australian Pb ores and the mean isotopic compositions of natural Pb in the samples. Linear regression lines are shown in solid line for the pre-1900 and dotted line for 1990–1996; (b) 3-isotope plot showing a shift with the time intervals.

Pb was massively injected into the Earth's atmosphere (Murozumi et al., 1969; McConnell and Edwards, 2008). Thus, our record appears to characterize a more regional feature of central Asia in comparison with a global scope.

4.2. Lead isotopic composition as tracer of source regions affecting natural Pb inputs

Fig. 4 shows the plot of $^{206}\text{Pb}/^{207}\text{Pb}$ versus $^{208}\text{Pb}/^{207}\text{Pb}$ for all samples. The $^{206}\text{Pb}/^{207}\text{Pb}$ and $^{208}\text{Pb}/^{207}\text{Pb}$ ratios of pre-anthropogenic Pb are well defined within the field of K-feldspars of Indian shield on which Mt. Everest is located, whereas the $^{206}\text{Pb}/^{207}\text{Pb}$ and $^{208}\text{Pb}/^{207}\text{Pb}$ ratios diverge from the ratios for Lhasa block in the Tibetan Plateau and Kohistan terrane of the northern Pakistan Himalaya characterized by lower ratios. This feature indicates that mineral dust from local sources is primarily responsible for the natural background Pb in the high altitude atmosphere of central Himalayas.

However, it is assumed that other potential dust sources could also affect the input of dust to the central Himalayas. In Fig. 4, a few data points are close to the isotopic composition of the Sahara Desert. This suggests that long range transport of Sahara dust may have become occasionally important in the central Himalayas, possibly due to the westerly jet in winter non-monsoon season (Thompson et al., 2000). In addition, the different potential source regions may be the arid regions of the Thar Desert and Indus-Gangetic Basin of northwestern India (Hegde et al., 2007). Recently, using a combined analysis of the Sr–Nd–Pb isotopic compositions in the shallow ice core at the same drilling site and backward air mass trajectories, it was reported that dust in the dirty layers originated mainly from local sources, while the Thar Desert and Indus-Gangetic Basin of northwestern India are attributed to a possible source of the particles in the non-dirty layers (Xu et al., 2009b).

4.3. Anthropogenic lead contamination and its possible sources for the post-1960s

Fig. 5 shows the relationships of EF values and $^{206}\text{Pb}/^{207}\text{Pb}$ ratios plotted against Sc concentrations for the post-1960s. The seasonal atmospheric circulation patterns that dominate in the central Himalayas are well characterized with respect to both monsoon and non-monsoon seasons (Fig. 1). During the summer monsoon season, air masses move from the south, whereas continental westerly winds prevail during the non-monsoon season (winter-spring). The highest concentrations of crustal elements in snow occur in spring,

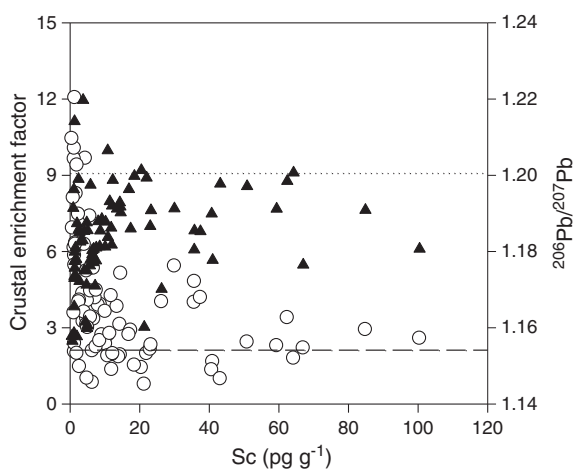


Fig. 5. Changes in crustal enrichment factors (open circles) and $^{206}\text{Pb}/^{207}\text{Pb}$ ratios (solid triangles) as a function of Sc concentrations for the post-1960s period. Also shown are long dashed line of mean EF value and dotted line of mean $^{206}\text{Pb}/^{207}\text{Pb}$ ratio for the pre-anthropogenic Pb.

resulting from a high influx of mineral dust coming from central Asia (Thompson et al., 2000; Kang et al., 2004).

Higher EFs and lower $^{206}\text{Pb}/^{207}\text{Pb}$ ratios tend to generally occur at relatively lower Sc concentrations. As previously reported (Lee et al., 2008; Hong et al., 2009; Kaspari et al., 2009), an anthropogenic enrichment of trace elements in the summer monsoon snow and ice was observed in the central Himalayas, suggesting South Asia as the most potential source regions. Air mass back trajectory analysis supported this speculation (Li et al., 2007). Despite such a general pattern of the inputs of air pollutants to the central Himalayas, however, the situation for Pb seems to be moderately different from other elements. In Fig. 5, enhanced EFs and $^{206}\text{Pb}/^{207}\text{Pb}$ ratios lower than the natural mean levels are also shown when Sc concentrations are relatively high. Based on similar transport and deposition of Pb with dust of local origin as indicated by our data and those from Xu et al. (2009b), this feature is likely to suggest that anthropogenic Pb from local sources could have reached the high altitude atmosphere in the central Himalayas even during the non-monsoon period.

A plot of $^{206}\text{Pb}/^{207}\text{Pb}$ versus $^{208}\text{Pb}/^{207}\text{Pb}$ for the post-1960s shows a trend moving toward less radiogenic values, with a deviation from a linear regression line of the natural Pb (Fig. 4b). An interesting shift is observed in a detailed overview of changes in the ratios over time. In Fig. 4b, the isotope ratios except for one data point in the 1960s are similar to those for the pre-anthropogenic Pb, indicating a comparatively negligible input of anthropogenic Pb during this time period. In the 1970s, more data points of lower Pb isotope ratios are placed outside the pre-anthropogenic ratios. Subsequently, a shift in the ratios is characterized by further less radiogenic values in the 1980s. The most distinct feature of changes in the isotopic compositions is then observed in the period 1990–1996. In those years, the spread in Pb isotopic ratios is very wide and a shift in the isotope ratios toward less radiogenic values is the most pronounced, with the least mean ratios of 1.178 for $^{206}\text{Pb}/^{207}\text{Pb}$ and 2.471 for $^{208}\text{Pb}/^{207}\text{Pb}$, respectively (Table 2). Temporal variations in both EFs and Pb isotope ratios shown in our samples reflect an increasing influence of less radiogenic Pb of anthropogenic origin during the corresponding periods.

As described before, South Asia is the most potential source regions. Among the major sources such as non-ferrous metal production, automobile and coal combustion, the most significant emission of Pb was due to the use of leaded gasoline in urban areas of South Asia including India, Bangladesh, Nepal and Pakistan before the introduction of unleaded gasoline as the cases for the developed countries (Biswas et al., 2003; Kadir et al., 2008; Singh and Singh, 2006; Thomas et al., 1999). In India, the largest contributor in South Asia, the Pb emission from leaded gasoline was larger by a factor of 4–5 than those from coal combustion and non-ferrous metals production between 1970 and the mid-1990s (Hong et al., submitted for publication).

Alkyl lead additives in gasoline used in India were exclusively supplied by the British company Associated Octel (Gulson et al., 2004). Their alkyl lead was usually characterized by relatively low ratios (1.06–1.10 of $^{206}\text{Pb}/^{207}\text{Pb}$ ratio), because Associated Octel used about 50–80% Australian Pb in alkyl lead production (Véron et al., 1999). Therefore, the tendency of the isotope ratios moving toward values typical for Australian Pb ores since the 1970s is likely mainly due to an input of less radiogenic Pb emitted from leaded gasoline in India. Interestingly, the only data point available for the isotopic composition of the Indian aerosol in 1995 is well located on the linear fit for the period 1990–1996 (Fig. 4a). This may support that gasoline Pb in India was the major source of anthropogenic Pb enrichment in the central Himalayas during a corresponding period. In addition, Bangladesh and Nepal could be a potential source region, because of air masses prevailing from the south to central Himalayas during the summer monsoon season and serious atmospheric Pb pollution due to automobile exhaust before banning leaded gasoline in those

countries in 1999 (Biswas et al., 2003). Although no data are available for the aerosol isotope ratios in Bangladesh and Nepal, the isotopic compositions in two countries are assumed to be probably similar to those in India, because of alkyl lead supplied by Associated Octel in South Asia (Bollhöfer and Rosman, 2001, 2002). In Fig. 4a, the isotopic composition of the aerosols collected in 1998–1999 in Pakistan, another possible source region, is placed between line of two end points and linear regression line for the period 1990–1996. Significantly lower isotope ratios of the Pakistan aerosols were attributed to gasoline Pb with the same source (Associated Octel) of alkyl lead (Bollhöfer and Rosman, 2001, 2002), because the phase-out of leaded gasoline was completed in Pakistan in 2002 (Singh et al., 2008). Air masses from Pakistan occasionally reach the sampling site (Xu et al., 2009b) and similar isotopic ratios fall between two lines (Fig. 4a). These facts suggest that a contribution from Pakistan is possible, but it might be small, because the isotopic compositions slightly diverge from the linear line of the period 1990–1996. As shown in Fig. 4a, the isotopic composition of the aerosols sampled in Sri Lanka in 1990 shows much less radiogenic ratios, probably reflecting the influence of alkyl lead supplied by Associated Octel (Mukai et al., 1993). Similar to the spread in Pb isotopic ratios in aerosols in Pakistan, isotopic ratio of Sri Lanka is shown to diverge from the linear line of the period 1990–1996, which probably suggests that a contribution from Sri Lanka is substantially minor. For comparison, an influence of Chinese leaded gasoline is assumed to be negligible, because of a deviation of their isotope ratios from a well defined alignment of all data for the post-1960s (Fig. 4a). From our data, it is plausible that a decrease in $^{206}\text{Pb}/^{207}\text{Pb}$ and $^{208}\text{Pb}/^{207}\text{Pb}$ ratios between 1970s and 1990s with a drastic decrease in 1990 to 1996 can be explained mainly by an increasing Pb emissions from leaded gasoline used in South Asia, particularly in India as well as probably Bangladesh and Nepal.

As for the contribution from non-ferrous metal production, it is likely that this contribution was insignificant, because the isotope ratios of Indian Pb ores are generally much lower than those of the samples for the post-1970s (Fig. 4a) and the amount of Pb emitted from non-ferrous metals production was relatively small compared to that from leaded gasoline (Hong et al., submitted for publication). A lack of information about Pb isotope ratios in coals used in India does not allow its contribution to be identified. However, coal consumption is assumed to be a minor source before the introduction of unleaded gasoline in South Asia (Hong et al., submitted for publication).

In Fig. 4b, most data points in the period 1997–2002 are characterized by a shift toward more radiogenic values, reflecting a decreasing influence of gasoline Pb or an increase in more radiogenic Pb inputs or both. The nationwide reduction of the Pb content in gasoline from 0.56 g/l to 0.15 g/l was completed in India in 1997 and then the ban of leaded gasoline usage in 2000 (Singh and Singh, 2006). Accordingly, the Pb content in gasoline was lowered from 0.8 g/l to 0.4 g/l by 1997 in Bangladesh and the phase-out of leaded gasoline was completed in Bangladesh and Nepal in 1999 (Biswas et al., 2003; Jha and Lekhak, 2003), which resulted in significant decrease in atmospheric Pb in urban areas of those countries (Biswas et al., 2003; Singh and Singh, 2006). Therefore, both more radiogenic isotope ratios and slight decrease in EFs in the period 1997–2002 (Table 2) are likely attributed to reducing Pb emissions from leaded gasoline in South Asia. In contrast, an influence of fossil fuel combustion is expected to increase during a corresponding period (Hong et al., submitted for publication). For instance, the annual emission of Pb from fossil fuel combustion to the atmosphere in 2000 was estimated to reach about 1200 tons, which corresponds to 65% of Pb emission from the use of leaded gasoline in India in 1990 (Hong et al., submitted for publication). Previous studies on the aerosol in urban cities support this situation that coal combustion became a potential major source of atmospheric Pb after the introduction of unleaded gasoline in

South Asia (Salam et al., 2003; Patel et al., 2008). Additionally, despite no data available on coals used in South Asia, the $^{206}\text{Pb}/^{207}\text{Pb}$ ratios in coals from major coal deposits worldwide are found to range between 1.15 and 1.24 (Díaz-Somoano et al., 2009), which are more radiogenic compared to low ratios in gasoline Pb. Taken together, a relative increase in the isotope ratios between 1997 and 2002 may thus be partly associated with an increase in Pb emission from fossil fuel combustion.

As shown in Fig. 4a, the ratios in Chinese coal are close to those in our samples, indicating a possible contribution of Chinese coal to the Pb levels in the central Himalayas. However, it is likely that such contribution could be insignificant, because the isotope ratios of Pb from Chinese leaded gasoline are clearly distinct from those in our samples corresponding to 1960–1996 when gasoline Pb was a significant Pb source (Fig. 4a). This speculation is supported by the prevailing wind regimes, which prefer to transport the airborne particulate from neighboring regions around the central Himalayas (Thompson et al., 2000; Xu et al., 2009b). Moreover, an investigation at a remote area in northwest China, a probable source region, reported similar $^{206}\text{Pb}/^{207}\text{Pb}$ ratios (Fig. 4a), interpreting an influence by long-range transported Pb aerosols from Russia and Kazakhstan (Cheng et al., 2007). However, it should be said that a possible contribution from Chinese coal cannot be completely discarded, because the isotopic composition of Chinese coal is substantially lying close to those in our samples. A significantly higher resolved record of Pb isotopic signatures is required to clarify a specific source from a mixture of anthropogenic Pb from a variety of sources and source regions.

4.4. Effectiveness of the phase out of leaded gasoline on atmospheric lead contamination in the central Himalayas

Worldwide experience of definite influence of the phase-out of leaded gasoline on Pb level in the atmosphere has been extensively documented by numerous literatures (Thomas et al., 1999). Because the reduction of Pb in gasoline started from 1997 and subsequently leaded gasoline was phased out by 2000 in South Asia (Biswas et al., 2003; Singh et al., 2006), significant decrease in Pb concentrations is expected to have occurred after 2000 (Hong et al., submitted for publication). A significant decrease in Pb concentration is shown in 2000–2002 with a mean of 68 pg g^{-1} (Table 1). However, this value is comparable to that for 1990–1996 (Table 2), when the primary source of Pb was gasoline Pb. In addition, mean EF value in 2000–2002 remains high (4.8), indicating a level of anthropogenic Pb enrichment similar to previous time period. The reasons for these high levels of both Pb concentrations and EFs in 2000–2002 could be inter-annual variations (Kaspari et al., 2009; Hong et al., submitted for publication) or resuspended/fugitive Pb left after Pb was eliminated from the gasoline (Begum et al., 2005) or an increase of Pb emissions from other sources such as coal and oil combustion, non-ferrous metal production, and the use of Pb in various industries (Begum and Biswas, 2008; Bollhöfer and Rosman, 2001; Patel et al., 2008). However, we note that our interpretation is indeed dependent upon five data points only corresponding to the period 2000–2002 with the high EF value (9.7) in the 1.30–1.40 m sample (Table 1). Further study will help to assess the effectiveness of the reduction of atmospheric Pb in the central Himalayas in response to the phase-out of leaded gasoline in South Asia.

5. Conclusion

Temporal variations in Pb isotope ratios in ice cores from Mt. Everest reflect historical changes in the source of Pb in the remote Himalayan atmosphere during the past 800 years from 1205 to 2002 AD. Our data show that the primary source of Pb from 1205 until 1960s was apparently mineral dust originated from local sources with sporadic inputs from Sahara desert and northwestern India. Subsequently, a

shift of Pb isotope signatures toward less radiogenic values indicates that anthropogenic Pb has had a significant influence on Pb inputs to the Himalayas. Leaded gasoline used in South Asia (especially India) appears the most prevalent atmospheric Pb source from the 1970s onward. Interestingly, the reduction of both Pb concentrations and EFs remained less prominent in the period 1997–2002, despite the regulation of leaded gasoline in South Asia during a corresponding time period. Such feature could be probably related to an increase in Pb emissions from other anthropogenic sources such as fossil fuel combustion and non-ferrous metal production by the accelerating industrialization in South Asia. Further study is required to substantiate this assumption in the future.

Acknowledgments

We thank all field personnel for the scientific expedition to Mt. Qomolangma (Everest) in 2002. This work was supported in Korea by KOPRI research grant (PP09010) and INHA University research grant (INHA-42819-01) and in China by grants 2007CB411501, 40825017, and SKLCS-ZZ-2008-06.

References

- Begum BA, Biswas SK, Kim E, Hopke PK, Khaliqzaman M. Investigation of sources of atmospheric aerosol at a hot spot area in Dhaka, Bangladesh. *J Air Waste Manage Assoc* 2005;55:227–40.
- Begum BA, Biswas SK. Trends in particulate matter (PM) and lead pollution in ambient air of Dhaka city in Bangladesh. *J Banglad Acad Sci* 2008;32:2155–64.
- Biswas SK, Tarafdar SA, Islam A, Khaliqzaman M, Tervahattu H, Kupiainen K. Impact of unleaded gasoline introduction on the concentration lead in the air of Dhaka, Bangladesh. *J Air Waste Manage Assoc* 2003;53:1355–62.
- Bollhöfer A, Rosman KJR. Isotopic source signatures for atmospheric lead: the Northern Hemisphere. *Geochim Cosmochim Acta* 2001;65:1727–40.
- Bollhöfer A, Rosman KJR. The temporal stability in lead isotopic signatures at selected sites in the Southern and Northern Hemispheres. *Geochim Cosmochim Acta* 2002;66:1375–86.
- Boutron CF, Görlich U, Candelone JP, Bolshov MA, Delmas RJ. Decrease in anthropogenic lead, cadmium and zinc in Greenland snows since the late 1960s. *Nature* 1991;353:153–6.
- Candelone JP, Hong S, Boutron CF. An improved method for decontaminating polar snow and ice cores for heavy metal analysis. *Anal Chim Acta* 1994;299:9–16.
- Candelone JP, Hong S, Pellone C, Boutron CF. Post industrial revolution changes in large scale atmospheric pollution of the Northern Hemisphere by heavy metals as documented in central Greenland snow and ice. *J Geophys Res* 1995;100 (D8):16605–16.
- Chen J, Tan M, Li Y, Zhang Y, Lu W, Tong Y, et al. A lead isotopic record of Shanghai atmospheric lead emissions in total suspended particles during the period of phasing out of leaded gasoline. *Atmos Environ* 2005;39:1245–53.
- Cheng H, Zhang G, Jiang JX, Li X, Liu X, Li J, et al. Organochlorine pesticides, polybrominated biphenyl ethers and lead isotopes during the spring time at the Waliguan Baseline Observatory, northwest China: implication for long-range atmospheric transport. *Atmos Environ* 2007;41:4734–47.
- Chisholm C, Rosman KJR, Boutron CF, Candelone JP, Hong S. Determination of lead isotopic ratios in Greenland and Antarctic snow and ice at picogram per gram concentrations. *Anal Chim Acta* 1995;311:141–51.
- Cummings GL, Richards JR. Ore lead isotope ratios in a continuously changing earth. *Earth Planet Sci Lett* 1975;28:155–71.
- Dean JR. *Methods for environmental trace analysis*. London: John Wiley&Sons Ltd; 2003. p. 51–2.
- Deb M, Thorpe RI, Cumming GL, Wagner PA. Age, source and stratigraphic implications of Pb isotope data for conformable, sediment-hosted, base metal deposits in the Proterozoic Aravalli–Delhi orogenic belt, northwestern India. *Precambrian Res* 1989;43:1–22.
- Díaz-Somoano M, Kylander ME, López-Antón MA, Suárez-Ruiz I, Martínez-Tarazona MR, Ferrat M, et al. Stable lead isotope compositions in selected coals from around the world and implications for present day aerosol source tracing. *Environ Sci Technol* 2009;43:1078–85.
- Gariépy C, Allègre CJ, Xu RH. The Pb-isotope geochemistry of granitoids from the Himalaya-Tibet collision zone: implication for crustal evolution. *Earth Planet Sci Lett* 1985;74:220–34.
- Gulson BL, Venkatesh T, Palmer J, D'Souza HS, Korsch M. Comparison of isotope dilution and a portable anodic stripping voltammetry device for blood lead measurements: source of lead in blood of female adults from Bangalore. *Aust J Chem* 2004;57: 979–82.
- Hegde P, Pant P, Naja M, Dumka UC, Sagar R. South Asian dust episode in June 2006: aerosol observations in the central Himalayas. *Geophys Res Lett* 2007;34:L23802.
- Hong S, Candelone JP, Patterson CC, Boutron CF. Greenland ice evidence of hemispheric lead pollution two millennia ago by Greek and Roman civilizations. *Science* 1994;265:1841–3.
- Hong S, Lluberas A, Rodriguez F. A clean protocol for determining ultralow heavy metal concentrations: its application to the analysis of Pb, Cd, Cu, Zn and Mn in Antarctic snow. *Korean J Polar Res* 2000;11:35–47.
- Hong S, Lee K, Hou S, Hur SD, Ren J, Burn LJ, et al. An 800-year record of atmospheric As, Mo, Sn, and Sb in central Asia in high-altitude ice cores from Mt. Qomolangma (Everest), Himalayas. *Environ Sci Technol* 2009;43:8060–5.
- Hong S, Lee K, Hur S.D., Hou S., Batbante C, Boutron CF, submitted for publication. Mt. Everest ice core record of atmospheric Cu, Zn, Cd, Pb, and Pb isotopes variations during the past 800 years, in: Pacyna, J., Namiesnik, J., Nriagu, J., Markert, B. (Eds.), *Progress in Environmental Science, Technology and Management*. Maralthe, Netherland.
- Jha PK, Lekhak HD. Air pollution studied and management efforts in Nepal. *Pure Appl Geophys* 2003;160:341–8.
- Kadir MM, Janjua NZ, Kristensen S, Fatmi Z, Sathikumar N. Status of children's blood levels in Pakistan: implication for research and policy. *Public Health* 2008;122:708–15.
- Kang S, Mayewski PA, Qin D, Sneed SA, Ren J, Zhang D. Seasonal differences in snow chemistry from the vicinity of Mt. Everest, central Himalayas. *Atmos Environ* 2004;38:2819–29.
- Kaspari S, Mayewski P, Kang S, Sneed S, Hou S, Hooke R, et al. Reduction in northward incursions of the South Asian Monsoon since 1400 AD inferred from a Mt. Everest ice core. *Geophys Res Lett* 2007;34:L16701.
- Kaspari S, Hooke R, Mayewski P, Kang S, Hou S, Qin D. Snow accumulation rate on Qomolangma (Mount Everest), Himalaya: synchronicity with sites the Tibetan Plateau on 50–100 year time scales. *J Glaciol* 2008;54:343–52.
- Kaspari S, Mayewski PA, Handley M, Osterberg E, Kang S, Sneed S, et al. Recent increases in atmospheric concentrations of Bi, U, Cs, S and Ca from a 350-year Mount Everest ice core record. *J Geophys Res* 2009;114:D04302.
- Khan MA, Stern RJ, Gribble RF, Windley BF. Geochemical and isotopic constraints on subduction polarity, magma sources, and palaeogeography of the the Kohistan intra-oceanic arc, northern Pakistan Himalaya. *J Geol Soc London* 1997;154: 935–46.
- Komárek M, Ettler V, Chrástný M, Mihaljević M. Lead isotopes in environmental sciences: a review. *Environ Int* 2008;34:562–77.
- Lee K, Hur SD, Hou S, Hong S, Qin X, Ren J, et al. Atmospheric pollution for trace elements in the remote high-altitude atmosphere in central Asia as recorded in snow from Mt. Qomolangma (Everest) of the Himalayas. *Sci Total Environ* 2008;404:171–81.
- Li C, Kang S, Cong Z. Elemental composition of aerosols collected in the glacier area on Nyainqentanglha Range, Tibetan Plateau, during summer monsoon season. *Chin Sci Bull* 2007;52:3436–42.
- Li C, Kang S, Zhang Q. Elemental composition of Tibetan Plateau top soils and its effect on evaluating atmospheric pollution transport. *Environ Pollut* 2009;157:2261–5.
- McConnell J, Edwards R. Coal burning leaves toxic heavy metal legacy in the Arctic. *Proc Natl Acad Sci USA* 2008;105:12140–4.
- Mukai H, Furuta N, Fujii T, Ambe Y, Sakamoto K, Hashimoto Y. Characterization of sources of lead in the urban air of Asia using ratios of stable lead isotopes. *Environ Sci Technol* 1993;27:1347–56.
- Mukai H, Tanaka A, Fujii T, Zeng Y, Hong Y, Tang J, et al. Regional characteristics of sulfur and lead isotope ratios in the atmosphere at several Chinese urban sites. *Environ Sci Technol* 2001;35:1064–71.
- Murozumi M, Chow TJ, Patterson CC. Chemical concentrations of pollutant lead aerosols, terrestrial dusts and sea salts in Greenland and Antarctic snow strata. *Geochim Cosmochim Acta* 1969;33:1247–94.
- Patel KS, Gupta S, Nava S, Lucarelli F. Lead particulate pollution in central India. *World Academy of Science, Engineering Technol* 2008;43:574–7.
- Planchon FAM, Boutron CF, Barbante C, Wolff EW, Cozzi G, Gaspari V, et al. Ultrasensitive determination of heavy metals at the sub picogram per gram level in ultraclean Antarctic snow samples by inductively coupled plasma sector field mass spectrometry. *Anal Chim Acta* 2001;450:193–205.
- Rosman KJR, Chisholm W, Boutron CF, Candelone JP, Görlich U. Isotopic evidence for the source of lead in Greenland snows since the late 1960s. *Nature* 1993;362:333–4.
- Rosman KJR, Chisholm W, Boutron CF, Candelone JP, Hong S. Isotopic evidence to account for changes in the concentration of lead in Greenland snow between 1960 and 1988. *Geochim Cosmochim Acta* 1994;58:3265–9.
- Rosman KJR, Chisholm W, Hong S, Candelone JP, Boutron CF. Lead from Carthaginian and Roman Spanish mines isotopically identified in Greenland ice dated from 600 B.C. to 300 A.D. *Environ Sci Technol* 1997;31:3413–6.
- Rosman KJR, Chisholm W, Boutron CF, Candelone JP, Jaffrezzo JL, Davidson CI. Seasonal variations in the origin of lead in snow at Dye 3, Greenland. *Earth Planet Sci Lett* 1998;160:383–9.
- Salam A, Bauer H, Kassin K, Ullah SM, Puxbaum H. Aerosol chemical characteristics of a mega-city in Southeast Asia (Dhaka-Bangladesh). *Atmos Environ* 2003;37:2517–28.
- Schwikowski M, Barbanche C, Doering T, Gaeggeler HW, Boutron CF, Schotterer U, et al. Post-17th-century changes of European lead emissions recorded in high-altitude Alpine snow and ice. *Environ Sci Technol* 2004;8:957–64.
- Shotyk W, Zheng J, Krachler M, Zdanowicz C, Koerner R, Fisher D. Predominance of industrial Pb in recent snow (1994–2004) and ice (1842–1996) from Devon Island, Arctic Canada. *Geophys Res Lett* 2005;32:L21814.
- Singh AK, Singh M. Lead decline in the Indian environment resulting from the petrol-lead phase-out programme. *Sci Total Environ* 2006;368:686–94.
- Singh A, Gangopadhyay S, Nanda PK, Bhattacharya S, Sharma C, Bhan C. Trends of greenhouse gas emissions from the road transport sector in India. *Sci Total Environ* 2008;390:124–31.
- Sun SS. Lead isotopic study of young volcanic rocks from Mid-ocean ridges, ocean island and island arcs. *Phil Trans Royal Soc London* 1980;A297:409–45.
- Tan MG, Zhang GL, Li XL, Zhang YX, Yue WS, Chen JM, et al. Comprehensive study of lead pollution in Shanghai by multiple techniques. *Anal Chem* 2006;78:8044–50.

- Thomas VM, Socolow RH, Fanelli JJ, Spiro TG. Effects of reducing lead in gasoline: an analysis of the international experience. *Environ Sci Technol* 1999;33:3942–8.
- Thompson LG, Yao T, Mosley-Thompson E, Davis ME, Henderson KA, Lin PN. A high-resolution millennial record of the South Asian monsoon from Himalayan ice cores. *Science* 2000;289:1916–9.
- Vallelonga P, Van de Velde K, Candelone JP, Ly C, Rosman KJR, Boutron CF, et al. Recent advances in measurement of Pb isotopes in polar ice and snow at sub-picogram per gram concentrations using thermal ionisation mass spectrometry. *Anal Chim Acta* 2002;453:1–12.
- Véron A, Flament P, Bertho ML, Alleman L, Flegal R, Hamelin B. Isotopic evidence of pollutant lead sources in Northwestern France. *Atmos Environ* 1999;33:3377–88.
- Xu J, Kaspari S, Hou S, Kang S, Qin D, Ren J, et al. Records of volcanic events since AD 1800 in the East Rongbuk ice core from Mt. Qomolangma. *Chinese Sci Bull* 2009a;54:1–6.
- Xu J, Hou S, Chen F, Ren J, Qin D. Tracing the sources of particles in the East Rongbuk ice core from Mt. Qomolangma. *Chinese Sci Bull* 2009b;54:1781–5.
- Zheng J, Shotyk W, Krachler M, Fisher D. A 15,800-year record of atmospheric lead deposition on the Devon Ice Cap, Nunavut, Canada: natural and anthropogenic enrichments, isotopic composition, and predominant sources. *Glob Biogeochem Cycles* 2007;21:GB2027.
- Zhu BQ, Chen YW, Peng JH. Lead isotope geochemistry of urban environment in the Pearl River Delta. *Appl Geochem* 2001;16:409–17.